

Merger History of Clustered Primordial Black Holes

Viktor Stasenko

National Research Nuclear University MEPhI, 115409 Moscow, Russia
MIREA — Russian Technological University, 119454 Moscow, Russia

E-mail: vdstasenko@mephi.ru

Abstract. Primordial black hole (PBH) binaries experience strong gravitational perturbations in the case of their initial clustering, which significantly affects the dynamics of their mergers. In this work, we develop a new formalism to account for these perturbations and track the evolution of the binary orbital parameters distribution. Based on this approach, we calculate the merger rate of PBH binaries and demonstrate that its temporal evolution differs greatly from that of isolated binary systems. Moreover, PBH clustering produces distinctive features in the stochastic gravitational-wave background: the canonical $2/3$ spectral slope transforms to $\Omega_{\text{gw}} \propto \nu^{-65/28}$ in a certain frequency band. These predictions can be probed in future gravitational wave observations, opening up new opportunities to test the clustering of PBHs and their contribution to dark matter.

Contents

1	Introduction	1
2	Primordial black hole clustering	2
3	Primordial black hole binaries	3
4	Perturbations of binaries	5
5	Primordial black hole merger rate	7
6	Stochastic gravitational wave background	11
7	Conclusion	13

1 Introduction

Progress in gravitational-wave astronomy has led to a surge of interest in primordial black holes (PBHs) — hypothetical black holes that may have formed in the very early Universe. [1, 2]. In recent years, the LIGO-Virgo-KAGRA collaboration has detected dozens of compact object merger events [3, 4]. Most of them are interpreted as mergers of black holes of astrophysical origin, but the primordial nature of a part of the detected events is also popular [5–12]. This interpretation is particularly valuable because it allows us to use gravitational-wave (GW) observations as a tool to impose constraints on the density of PBHs in the Universe. Moreover, many other independent observations have imposed additional constraints, but primordial black holes remain a viable candidate for dark matter [13] — one of the central problems of modern fundamental science.

It is traditionally considered that PBH binaries are formed at the radiation-dominated stage of the Universe evolution due to fluctuations in their spatial distribution [6, 14]. Despite a well theoretical elaboration of this scenario, quantitative estimates of the merger rate face uncertainties. The main difficulties are related to various factors that affect the binary systems: in particular, the interaction of the binaries with the dark matter halo that forms around them [15–18]; perturbations of black hole pairs in early structures arising from their natural Poisson clustering [10, 19–24]; and other possible effects.

In this paper, we consider an alternative scenario assuming an initially clustered birth of PBHs. In this case, the statistics of PBH pairs is formally constructed similarly to the model of their random distribution in space [6, 14]. However, in the case of strong clustering, the key difference is that the PBH binaries appear to be embedded in a dense environment. In such conditions they are subjected to continuous gravitational perturbations from the surrounding single PBHs. In this paper we develop a new formalism describing how these perturbations affect mergers of PBH binaries. Our calculations show that this process leads to a significantly different temporal evolution of the merger rate compared to the prediction for pairs of PBHs without initial clustering. In particular, intense perturbations can both destroy the existing binary systems and significantly modify the orbital parameters of the surviving pairs, increasing their lifetime. These effects have a significant impact on the spectral characteristics of the stochastic GW background, which integrates the contribution

of black hole mergers over cosmological history to the GW energy density in the Universe. The results have important observational implications for next generation of gravitational-wave experiments such as LISA [25], TianQin [26], Einstein Telescope [27, 28] and other proposed projects. Their expected sensitivity will allow both the detection of individual black hole merger events at high redshifts and the measurement of the gravitational-wave background over a wide frequency range, providing a test of the PBH idea.

The paper is organized as follows. Section 2 develops the simple theoretical formalism for PBH cluster formation. In Section 3, we analyze the formation of PBH binaries during the radiation-dominated era of the Universe. Section 4 provides both qualitative analysis of the perturbation processes affecting binary systems and analytical estimates for the parameters of binaries undergoing perturbations. Section 5 presents our calculations of the PBH merger rate incorporating these perturbation effects. The implications of our results for the stochastic gravitational wave background are discussed in Section 6. Finally, Section 7 summarizes our main findings.

2 Primordial black hole clustering

A number of theoretical models predict that the formation of PBHs is accompanied by their strong spatial clustering, which has been shown, for example, in the works [29–36]. The key idea is that in this case there must exist regions in the Universe with locally enhanced density of PBHs $\delta_{\text{PBH}} = \rho_{\text{PBH}}/\rho_{\text{DM}} > 0$, which are isocurvature fluctuations. The value δ_{PBH} is model-dependent, but in our consideration we consider it a free parameter, the specific choice of which determines the moment of gravitational detachment of the cluster from the Hubble flow. We parametrize the fraction of PBHs in the dark matter composition in the traditional way $f = \Omega_{\text{PBH}}/\Omega_{\text{DM}}$. Moreover, for clustering $\delta_{\text{PBH}} > f$ must be fulfilled, the case $\delta_{\text{PBH}} = f$ corresponds to the spatially random birth of PBHs in the Universe.

The formation of gravitationally bound structures occurs when the relative density contrast reaches a value on the order of unity $\delta\rho/\rho \sim 1$. In the radiation-dominated epoch, the radiation density falls as $\rho_r = \rho_{\text{eq}}(s/s_{\text{eq}})^{-4}$, and the density of PBH (like dark matter) $\rho_{\text{PBH}} = \rho_{\text{eq}}\delta_{\text{PBH}}(s/s_{\text{eq}})^{-3}$, where s_{eq} is the scale factor at the moment of matter-radiation equality t_{eq} . At the present moment, the scale factor is normalized to unit $s_0 = 1$. At the stage of radiation dominance the isocurvature fluctuations are “frozen”, so the moment of formation can be determined from the condition $\rho_r \sim \rho_{\text{PBH}}$. Hence we obtain an estimate for the moment of cluster formation $\delta_{\text{PBH}} \sim s_{\text{eq}}/s_f$. In this way, a gravitationally bound structure is formed, separated from the Hubble expansion, consisting of PBHs and dark matter particles with density $\rho = B\rho_{\text{eq}}\delta_{\text{PBH}}^3(1 + \delta_{\text{PBH}})$, where the constant B is determined from the numerical solution of this problem and will be given below. In the case $\delta_{\text{PBH}} < 1$, cluster formation occurs at the dust stage of the Universe, when structures form due to gravitational instability. During this period, small density fluctuations grow in the linear regime as $\delta\rho/\rho \propto s$, which leads to a similar estimate for the moment of cluster formation $\delta_{\text{PBH}} \sim s_{\text{eq}}/s_f$. The analysis in [37] demonstrates that in both cases the density is well described by a simple expression

$$\rho \approx 140 \rho_{\text{eq}} \delta_{\text{PBH}}^3 (1 + \delta_{\text{PBH}}). \quad (2.1)$$

The density of the PBHs will be $\rho_{\text{PBH}} \approx 140 \delta_{\text{PBH}}^4 \rho_{\text{eq}}$. Here $\rho_{\text{eq}} = 2\Omega_{\text{DM}}\rho_{\text{crit}}(1 + z_{\text{eq}})^3$, $z_{\text{eq}} = 3402$ is the redshift matter-radiation equality and $\rho_{\text{crit}} = 3H_0^2/8\pi G$ is the critical

density of the Universe. The expression for the Hubble parameter is

$$H^2(z) = H_0^2 \left[\Omega_\Lambda + \Omega_M(1+z)^3 + \Omega_r(1+z)^4 \right]. \quad (2.2)$$

In our calculations we use the cosmological parameters $H_0 = 67.4 \text{ km s}^{-1} \text{ Mpc}^{-1}$, $\Omega_\Lambda = 0.69$, $\Omega_M = 0.31$, $\Omega_r = 5.4 \times 10^{-5}$ [38]. All numerical calculations are carried out for PBHs with mass $m = 10 M_\odot$, which is within the mass range of the registered LIGO-Virgo-KAGRA events. However we also provide analytical expressions of our results that allow us to generalize the findings to the case of arbitrary masses of the PBHs. Also, throughout the paper we adopt the approximation $\Omega_{\text{DM}} = \Omega_M$, since taking into account the baryonic component will only make minor corrections to our results.

3 Primordial black hole binaries

During the radiation-dominated stage, the PBHs form gravitationally bound pairs. This occurs because at some moment of time $t_d < t_{\text{eq}}$ the local density of two PBHs will exceed the radiation density $\rho_r(t_d)$. In this sense, the situation is completely analogous to the formation of clusters discussed in the previous section. To describe this process, we introduce the mean physical distance between the PBHs at the moment t_{eq}

$$\bar{x} = \left(\frac{m}{\rho_{\text{PBH}}} \right)^{1/3} = \frac{1}{s_{\text{eq}} \delta_{\text{PBH}}^{1/3}} \left(\frac{m}{\Omega_{\text{DM}} \rho_{\text{crit}}} \right)^{1/3}. \quad (3.1)$$

Since the radiation density falls as $\rho_r \propto s^{-4}$, the moment of gravitational detachment of the pair is determined by the following expression

$$\frac{m}{R^3} = \rho_r(t_d) = \rho_{r,\text{eq}} \left(\frac{s_{\text{eq}}}{s_d} \right)^4, \quad (3.2)$$

here $R = x s_d / s_{\text{eq}}$ is the physical distance between the PBHs at the moment t_d , and x is the distance at the moment t_{eq} . Thus, the moment of formation of the binary system is determined as

$$\frac{s_{\text{eq}}}{s_d} = \delta_{\text{PBH}} \left(\frac{\bar{x}}{x} \right)^3. \quad (3.3)$$

For the detachment moment in the described formalism, there are two natural bounds: $s_d < s_{\text{eq}}$ in the case $\delta_{\text{PBH}} < 1$ and $s_d < s_{\text{eq}} / \delta_{\text{PBH}}$ when $\delta_{\text{PBH}} > 1$. The second condition arises because the gravitational detachment of the pair from the Hubble flow must occur before the formation of the cluster. Taking this into account, as well as the fact that $x < \bar{x}$, we conclude that pairs are formed only by those PBHs whose distance between them satisfies the relation $x < \bar{x} \delta_{\text{PBH}}^\gamma$, where γ is used to parameterize two possible clustering modes: $\gamma = 1/3$ for $\delta_{\text{PBH}} < 1$ and $\gamma = 0$ for the case $\delta_{\text{PBH}} > 1$.

After detachment from the expansion of the Universe, the PBHs avoid a head-on collision and move in an elliptical orbit around each other because the surrounding PBHs generate angular momentum due to tidal forces. Here, for simplicity, we consider only the main contribution from the nearest PBH, the distance to which we denote by y , and the condition $x < y < \bar{x}$ must be satisfied. We follow the formalism of work [6] and take the probability distribution over x and y to be flat in three-dimensional space

$$dP = \frac{9}{\bar{x}^6} x^2 y^2 dx dy. \quad (3.4)$$

The major and minor axes of the PBH binary are determined by the equations

$$a = \frac{\alpha x}{\delta_{\text{PBH}}} \left(\frac{x}{\bar{x}}\right)^3, \quad b = \beta a \left(\frac{x}{y}\right)^3, \quad (3.5)$$

further, the coefficients α and β are taken to be equal to unity. The eccentricity of a binary is defined as $e = \sqrt{1 - b^2/a^2}$, but it is more convenient to use the dimensionless angular momentum $j = \sqrt{1 - e^2} = (x/y)^3$ instead. To characterize the PBH binaries it is convenient to transform to the variables a and j in the distribution (3.4)

$$dP = \frac{3}{4} \left(\frac{\delta_{\text{PBH}}}{\bar{x}}\right)^{3/2} \frac{\sqrt{a}}{j^2} da dj, \quad (3.6)$$

where the variables vary in the range $0 < a < \bar{x} \delta_{\text{PBH}}^{4\gamma-1}$, $(a\delta_{\text{PBH}}/\bar{x})^{3/4} < j < 1$. The lower bound on j corresponds to the fact that the distance to the third PBH is maximized $y = \bar{x}$. From the distribution of (3.6) we can see that PBH binaries mainly have small angular momenta at formation, i.e., their orbits are strongly elongated. Due to the emission of gravitational waves a pair of black holes of the same mass m merge in time [39]

$$t_{\text{gw}} = \frac{3c^5 a^4 j^7}{170G^3 m^3}. \quad (3.7)$$

Let us now determine the characteristic initial values of the parameters of the PBH binaries merging by a time t_{mer} . As noted above, the distribution (3.6) is maximal at small j , so the characteristic value of the angular momentum can be estimated as $j_{\text{ch}} \sim j_{\text{min}} = (a\delta_{\text{PBH}}/\bar{x})^{3/4}$. Then from the binary merger time (3.7) we obtain the characteristic value for the major semiaxis

$$a_{\text{ch}} = \left(\frac{170G^3 m^3 t_{\text{mer}}}{3c^5}\right)^{4/37} \left(\frac{\bar{x}}{\delta_{\text{PBH}}}\right)^{21/37} \approx 42 \delta_{\text{PBH}}^{-28/37} \left(\frac{m}{M_{\odot}}\right)^{19/37} \left(\frac{t_{\text{mer}}}{t_0}\right)^{4/37} \text{ au}, \quad (3.8)$$

where $t_0 = 13.8$ Gyr is the age of the Universe. Since a_{ch} depends very weakly on t_{mer} , almost all merging binaries at not too far cosmological distances are characterized by approximately the same value of the large semi-axis. Now let us compare the obtained value with the maximum possible major semiaxis. In the case of $\delta_{\text{PBH}} < 1$, the limiting value of a_{max} corresponds to the average distance between the PBHs at $\delta_{\text{PBH}} = 1$, which is $a_{\text{max}} \sim 10^4$ au. In the case $\delta_{\text{PBH}} > 1$, we get $a_{\text{max}} \sim 10^4 \delta_{\text{PBH}}^{-4/3}$ au. Thus, all PBH binaries merging by the modern epoch formed gravitationally bound pairs long before the transition to the stage of matter dominance (or before the formation of the cluster t_f at $\delta_{\text{PBH}} > 1$). Substituting the found expression for the semi-major axis (3.8) into $j_{\text{min}} = (a\delta_{\text{PBH}}/\bar{x})^{3/4}$ one can determine the characteristic value of the angular momentum of the binaries

$$j_{\text{ch}} \approx 0.01 \delta_{\text{PBH}}^{16/37} \left(\frac{m}{M_{\odot}}\right)^{5/37} \left(\frac{t_{\text{mer}}}{t_0}\right)^{3/37}. \quad (3.9)$$

Thus, PBH binaries are characterized by small angular momenta $j \ll 1$, which will be used later in the analysis of the interaction of such binaries with single PBHs.

4 Perturbations of binaries

Since PBH binaries are embedded in clusters, they are subjected to gravitational perturbations by single black holes. Because of this, the orbital parameters of the binaries change. The key parameter determining the outcome of such interactions is the hardness of the binary. A system is considered hard if its binding energy E_b exceeds by absolute value the characteristic kinetic energy of black holes in the cluster $\sim m\sigma^2$. In terms of orbital parameters this condition corresponds to the constraint on the large semi-axis

$$a < a_h = \frac{Gm}{2\sigma^2} \approx 4.4 \left(\frac{\sigma}{10 \text{ km s}^{-1}} \right)^{-2} \left(\frac{m}{M_\odot} \right) \text{ au}, \quad (4.1)$$

Binary systems with large semi-major axis $a > a_h$ are classified as soft, otherwise — rigid binaries. According to the classical Heggi-Hill law, such hard binaries tend to become harder when interacting with single objects ($|E_b|$ increases), while soft ones become softer [40, 41].

The comparison of the equations (3.8) and (4.1) shows that when $\delta_{\text{PBH}} \sim 1$ and the velocity dispersion $\sigma \sim 10 \text{ km s}^{-1}$ the characteristic binaries (3.8) are soft, so they will become even softer (or even destroy) as a result of perturbations. Moreover, since their angular momentum $j \ll 1$, it will mainly increase under the action of perturbations. This statement is also true for hard binaries with large eccentricities. The physical reason for this behavior is that the angular momentum distribution from the initial state (3.6) tends to the thermal one, for which $dP/dj \propto j$. The significant growth of the angular momentum was also confirmed by numerical modeling of such interactions in the work [20]. The increase of the angular momentum, in turn, leads to a significant increase of the lifetime of the binary. In particular, the increase of the angular momentum from the characteristic value j_{ch} to $j \sim 1$ causes the merger time to increase by a factor of $\sim 10^{14}$. Therefore, binaries that form on highly eccentric orbits, under the influence of perturbations, increase the time to merger by many orders of magnitude.

A different dynamics is expected for binary systems on nearly circular orbits. In their case, the perturbations will keep the angular momentum at $j \sim 1$. This makes such binaries “stable”, i.e. their merger time is practically unchanged by perturbations. Although hard binaries under the action of perturbations should still become harder, with a corresponding decrease of the merger time. However, it is difficult to quantitatively account for this effect because the hard binaries are eventually ejected from the cluster. Although predicting the orbital parameter distribution of the ejected binaries is of interest, the bulk of the binaries in the cluster still have small angular momenta. Therefore, in our calculations we restrict ourselves to the approximation in which the near circular binaries with $j > j_{\text{cut}}$ are considered stable: their orbital evolution and merger time are assumed to be unchanged. As a threshold value we take $j_{\text{cut}} = 1/2$; as will be seen below, the variation of this parameter does not significantly affect the main results of our work.

Let us now pass to the description of the perturbation of binary systems. The cross section of the approach of a binary, considered as a point object, and a single black hole to the distance r_p (pericenter of the orbit) is defined by the expression

$$\Sigma_p = \pi r_p^2 \left(1 + \frac{6Gm}{r_p v^2} \right), \quad (4.2)$$

here v — the relative velocity between the binary and single PBH at infinity. In our simplified model it is assumed that, as a result of a single act of hard scattering, the angular momentum

of the binary increases to $j \sim 1$ and hence its merger time increases significantly. To define hard scattering we use a simple criterion, which is that this distance of minimum approaching is equal to the major semiaxis $r_p = a$. The probability of such interactions is determined by the mean free time $\tau^{-1} = \rho_{\text{PBH}} \langle \Sigma_p v \rangle / m$. Assuming the Maxwell distribution of PBHs velocities in the cluster with dispersion σ , and after averaging over the relative velocities, we obtain the characteristic perturbation time of orbital parameters of PBH binaries

$$\tau^{-1} = \frac{2\sqrt{2\pi}}{m} 140 \rho_{\text{eq}} \delta_{\text{PBH}}^4 \sigma a^2 \left(1 + \frac{3Gm}{a\sigma^2} \right), \quad (4.3)$$

where the density of black holes in the cluster is $\rho_{\text{PBH}} \approx 140 \delta_{\text{PBH}}^4 \rho_{\text{eq}}$ (see Section 2). First of all, let us estimate the perturbation time of the characteristic binaries (3.8) merging in the modern epoch. As an example, we consider the case of the PBH with mass $m = 10 M_\odot$ with clustering parameter $\delta_{\text{PBH}} = 1$ and velocity dispersion $\sigma = 10 \text{ km s}^{-1}$. The perturbation time is estimated to be $\tau \approx 0.6 \text{ Myr}$, and since the semimajor axis of typical binaries (3.8) depends weakly on the merger time, it can be concluded that typical binaries are subject to perturbation for almost the entire cosmological history after their formation. Let us now consider the case of binaries in a circular orbit and with coalescence time t_0 . At the time of formation, the semimajor axis of such a binary should be $a \approx 0.8 \text{ au}$, and their perturbation time turns out to be $\tau \approx 2 \text{ Gyr}$. Note that for a cluster with velocity dispersion $\sigma > 75 \text{ km s}^{-1}$ these binaries turn out to be even soft. These estimates show that in the considered example all binaries that potentially produce observable GW signals are perturbed in clusters. In the case of earlier time scales $< t_0$ or with decreasing δ_{PBH} and PBH masses, the perturbations affect only a certain fraction of all binaries, namely only sufficiently wide binaries are subject to perturbations.

Let us now consider binaries with some merger time t_{mer} . Using Eq. (3.7), we express the major semiaxis through t_{mer} and angular momentum j to obtain the perturbation time $\tau(t_{\text{mer}}, j)$. The binaries with $\tau > t_{\text{mer}}$ merge before a significant perturbation, while in the opposite case at $\tau < t_{\text{mer}}$ the perturbation by a third black hole leads to an increase of the binary merger time. The angular momentum defining the boundary between these regimes is found from the solution of the equation $\tau(t, j_p) = t$:

$$j_p = 141 Gm \left(\frac{\rho_{\text{eq}} \delta_{\text{PBH}}^4 t^{5/4}}{m \sigma c^{5/4}} \right)^{4/7} \approx 0.28 \delta_{\text{PBH}}^{16/7} \left(\frac{\sigma}{10 \text{ km s}^{-1}} \right)^{-4/7} \left(\frac{m}{M_\odot} \right)^{3/7} \left(\frac{t}{\text{Gyr}} \right)^{5/7}, \quad (4.4)$$

where we used the gravitational focusing approximation in the cross section (4.2). As can be seen from the comparison of the Eqs. (3.9) and (4.4), most of the binaries that would merge in the contemporary Universe are perturbed since $j_p \gg j_{\text{ch}}$. Thus, a constraint on the angular momentum of merging binaries $1 < j < j_p$ arises, as is clearly demonstrated by Fig. 1. Let us now define the moment of time t_{sup} , starting from which the characteristic binaries are subject to perturbations, as a solution to the equation $\tau(a_{\text{ch}}) = t$:

$$t_{\text{sup}} \approx \frac{4.1 \text{ Myr}}{\delta_{\text{PBH}}^{120/41}} \left(\frac{\sigma}{10 \text{ km s}^{-1}} \right)^{37/41} \left(\frac{m}{M_\odot} \right)^{-19/41}. \quad (4.5)$$

Alternatively, this moment can be defined as the intersection of the j_p and j_{min} curves, which is also reflected in Fig. 1. For $t < t_{\text{sup}}$, the merger time t_{mer} turns out to be shorter than the perturbation time τ even for binaries with the largest possible semimajor axis. However, for $t > t_{\text{sup}}$, the merger suppression mechanism comes into play due to gravitational perturbations of the binaries by the surrounding PBHs.

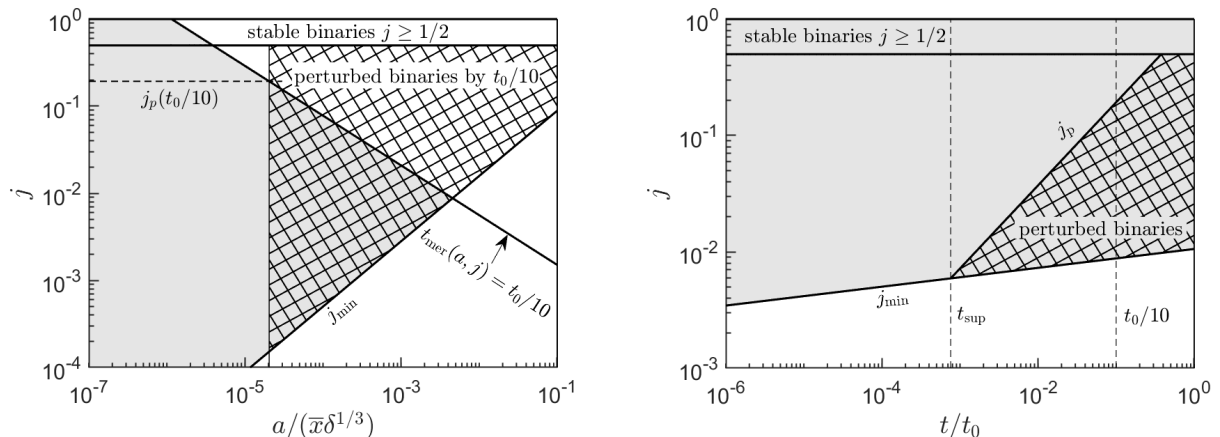


Figure 1. The example of the orbital parameter space of PBH binaries with $\delta_{\text{PBH}} = 0.5$, $\sigma = 10 \text{ km s}^{-1}$ and $m = 10 M_{\odot}$. Left: Binaries merging by time $\leq t_0/10$ are shaded in gray. The hatched area schematically shows binaries that have been perturbed at the same time, for which the semimajor axis exceeds the value given by $\tau(a) = t_0/10$. For reasons given in the text, perturbations of binaries with a nearly circular orbit ($j \geq 1/2$) are assumed not to affect their merger time. The dashed horizontal line indicates the critical angular momentum of binaries j_p (4.4), separating tight systems that avoid perturbation to $t_0/10$ and wide perturbed binaries. Right: Similar to the left parameter space, but on the (t, j) plane, where the transformation from a to t is done using Eq. (3.7). At fixed time t , the merging binaries have angular momenta from j_{min} to 1. However, systems with small angular momenta (corresponding to wide binaries) are perturbed, leading to an effective constraint from below on the value of j_p .

5 Primordial black hole merger rate

The perturbations of PBH binaries lead to their dynamical decrease: soft binaries are destroyed, and hard binaries switch to an orbit with angular momentum $j \sim 1$, which increases their merger time to values much larger than the age of the Universe t_0 . The key fact for this paper is that the perturbed binaries actually “drop out” from the merger process. This can be described as a continuous time evolution of the initial distribution (3.6) in orbital parameters

$$dP = \frac{3}{4} \left(\frac{\delta}{\bar{x}} \right)^{3/2} \frac{\sqrt{a}}{j^2} S(t, j, a) da dj, \quad (5.1)$$

where S is the suppression factor taking into account the decrease of the amount of merging binaries in time. Physically, it corresponds to the perturbation probability of the binary system and in our model is taken in the following simplified form

$$S(t, j, a) = \begin{cases} \theta(j_{\text{cut}} - j)e^{-t/\tau} + \theta(j - j_{\text{cut}}) & \text{if } a \leq a_h, \\ e^{-t/\tau} & \text{if } a > a_h, \end{cases} \quad (5.2)$$

where θ is Heaviside step function, a_h is the semimajor axis separating the hard and soft binaries defined by Eq. (4.1) and $j_{\text{cut}} = 1/2$ is the angular momentum above which the binaries are stable with respect to perturbations. The presented form of the suppression factor is physically explained in the previous section. Note that the influence of the initial

clustering of PBHs on their merger rate was also considered in Refs. [42–45], but without taking into account the perturbations of the binaries.

To determine the merger rate, it is convenient to transform from the semimajor axis variable a to time t using Eq. (3.7). Then the differential probability of a merger per unit time is given by

$$\frac{dP}{dt} = \frac{3}{16} \frac{\delta_{\text{PBH}}^2}{T} \left(\frac{t}{T}\right)^{-5/8} \int_{j_{\text{min}}}^1 j^{-37/8} S(t, j) dj, \quad (5.3)$$

where the lower limit is defined as $j_{\text{min}} = (t/T)^{3/37} \delta_{\text{PBH}}^{16/37}$ (which is also equivalent to Eq. (3.9)), and

$$T = \frac{3c^5 \bar{x}^4 \delta_{\text{PBH}}^{4/3}}{170G^3 m^3} \sim 10^{34} \left(\frac{m}{M_\odot}\right)^{-5/3} \text{ yr} \quad (5.4)$$

physically corresponds to the merger time of a PBH binary in a circular orbit with the maximum possible semi-major axis in the case of $\delta_{\text{PBH}} = 1$. The comoving merger rate of PBHs is determined by the expression

$$\mathcal{R} = \frac{f\Omega_{\text{DM}}}{m} \frac{3H_0^2}{8\pi G} \frac{dP}{dt}, \quad (5.5)$$

where the second fraction is the critical density ρ_{crit} and after numerical integration of Eq. (5.3) we obtain the time dependence of the merger rate, which is shown in Fig. (2). Note that we normalized all results here by f to exclude the dependence on the fraction of PBHs in dark matter. One can see that the merger rate at $t \ll t_0$ follows the dependence known for the case of unclustered PBHs [10]¹, the explanation is that the binaries have not yet begun to perturb, i.e. $S = 1$ and integration of the power function in Eq. (5.3) easily gives this answer. The merger rate then drops sharply at $t > t_{\text{sup}}$, with this behavior depending on the velocity dispersion in the cluster, as can be seen by comparing the purple dashed line and the solid lines.

To analyze the obtained result, we derive an approximate expression for the merger rate in the time region where the suppression factor is of the form $S = e^{-t/\tau(j,t)}$. Also for the beginning we will consider that the dispersion of velocities of black holes in the cluster is insignificant, i.e. the second term of gravitational focusing in the cross section (4.3) is the main one. As can be seen from Fig. (1), the main contribution to the integral (5.3) comes from the binaries with angular momenta $j \gtrsim j_p$. Numerical analysis shows that a good approximation is achieved by truncating the integral (5.3) from below at the value $j = 0.82 j_p$, and the suppression factor in the integration region can be neglected $e^{-t/\tau(j,t)} \rightarrow 1$. After the corresponding calculations we obtain

$$\mathcal{R} \approx \frac{1.8 \times 10^6}{\text{yr Gpc}^3} f \delta_{\text{PBH}}^{-44/7} \left(\frac{t}{10^8 \text{ yr}}\right)^{-45/14} \left(\frac{m}{M_\odot}\right)^{-27/14} \left(\frac{\sigma}{10 \text{ km s}^{-1}}\right)^{29/14}. \quad (5.6)$$

This dependence is shown by the red dotted line in Fig. (2), from which we can see that the derived expression indeed approximates well the merger rate at $t > t_{\text{sup}}$. Let us now consider the limiting case of a cluster with huge velocity dispersion. In this case, the cross

¹Although we note that the effects of natural Poisson clustering of PBHs at the matter dominated stage slightly modify this dependence, but they are valid at the fraction of PBHs in the dark matter composition $f \gtrsim 0.01$ [23]

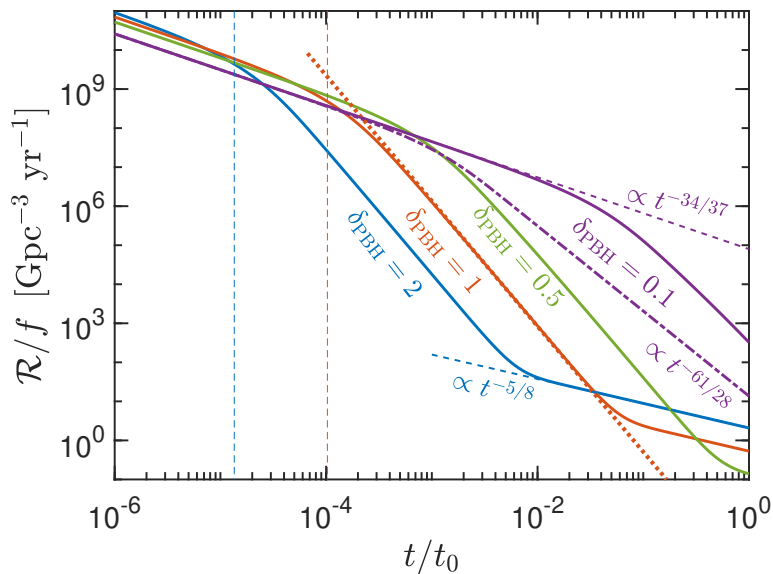


Figure 2. Time evolution of the merger rate for different values of the density contrast δ_{PBH} and velocity dispersion in the cluster $\sigma = 10 \text{ km s}^{-1}$. The purple dashed line shows the case of a cluster with $\sigma = 10^3 \text{ km s}^{-1}$ and $\delta_{\text{PBH}} = 0.1$. The red dotted line shows the analytical estimate of the merger rate given by Eq. (5.6). The vertical dashed lines show the moment of time t_{sup} , determined by Eq. (4.5), for $\delta_{\text{PBH}} = 2$ and $\delta_{\text{PBH}} = 1$, respectively.

section (4.2) becomes the geometric $\Sigma \propto a^2$. Using Eqs. (3.7) and (4.3) we obtain that the characteristic time of the perturbations scales as $\tau \propto t^{-1/2} j^{7/2}$. As in Sec. 4, determining the limiting angular momentum $\tau(t, j_p) = t$ leads to the following relation $j_p \propto t^{3/7}$. Truncating the integral (5.3) from below at angular momentum $\sim j_p$ (similar to the derivation Eq. (5.6)) gives the time dependence of the merger rate $\mathcal{R} \propto t^{-61/28}$. Note that in this case the power-law decay of the merger rate will change to exponential over time when the condition $j_p(t) = 1$ is reached, as follows from Eq. (5.2). This is due to the fact that binaries with a sufficiently long lifetime are soft in the cluster. That is, even pairs of PBHs in circular orbits (and even more so in elliptical orbits) will be destroyed due to perturbations, which is also seen in Fig. 3 in the region of $\delta_{\text{PBH}} > 1$ and $\sigma > 100 \text{ km s}^{-1}$.

Let us now turn to the discussion of larger time scales, where the merger rate experiences a sharp change in slope and comes to a dependence $\mathcal{R} \propto t^{-5/8}$. This result is more of an artifact of our model rather than a physical effect. This behavior arises from the specific form of the suppression factor (5.2), where we assume that the orbital parameters of binaries with sufficiently large angular momenta $j > j_{\text{cut}}$ do not change under perturbations. Then it is this region of angular momenta that will give the dominant contribution to the integral (5.3), so it is evaluated by a dimensionless constant. The time dependence arises only from the pre-integral factor, which explains the result. Moreover, changing the value of j_{cut} will only affect the amplitude of the merger rate, not its logarithmic slope. As noted in Section 4, a correct description requires taking into account the change in the distribution of the orbital parameters of the binaries under perturbations. Under the assumption that the distribution near large angular momenta takes the power-law form $dP/dj \propto j^k$, the merger rate will

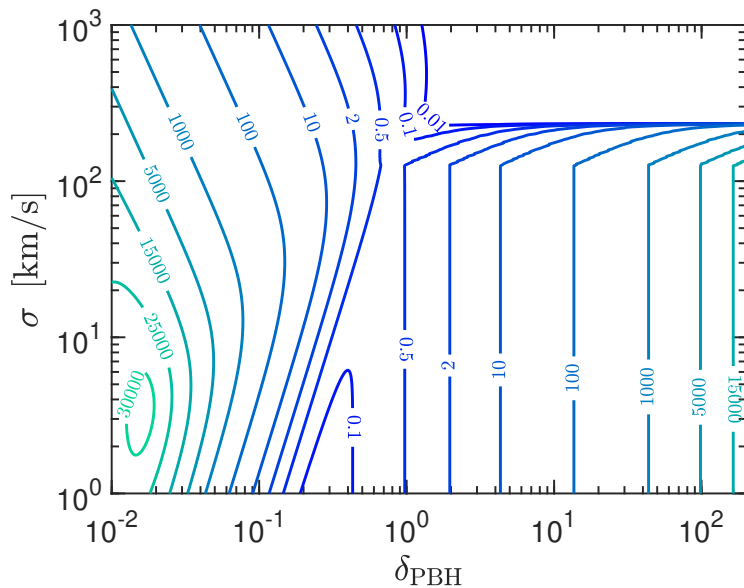


Figure 3. Contour plot of the modern merger rate of PBH binaries \mathcal{R}_0 (is shown on the curves in $[\text{Gpc}^{-3} \text{ yr}^{-1}]$ units.) calculated for the PBH fraction $f = 1$ for different clustering parameters δ_{PBH} and the velocity dispersion σ in the cluster, the PBH mass $m = 10 M_{\odot}$. The regions below the LIGO-Virgo-KAGRA merger rate $\mathcal{R}_0 = 18 \div 44 \text{ Gpc}^{-3} \text{ yr}^{-1}$ [3] formally allow for an explanation of dark matter through the PBHs (although other observations impose additional constraints [13]). For the remaining cases, $f < 1$ is required (also $f < \delta_{\text{PBH}}$ must be satisfied), which corresponds to a partial contribution of PBHs to dark matter.

vary as $\mathcal{R} \propto t^{(k-6)/7}$ [46], with $k = 1$ corresponding to the thermal distribution. Thus, in the physically realistic case, we expect the merger rate to also vary only slightly with time. However, the main result of this work is that there is a time window in which there is a sharp drop in the merger rate, which significantly diverges from the predictions of models in which the PBHs are initially distributed according to a Poisson law in space. This provides an opportunity to test the clustering of PBHs in future GW observations.

As noted above, perturbations of binaries with small eccentricities (almost circular orbits) make them harder, hence the merger time will decrease and therefore the merger rate of such binaries will increase. Therefore, our results in Fig.2 for $\delta_{\text{PBH}} > 1$ and time scales $\sim t_0$ (in this case, binaries with $j > j_{\text{cut}}$ merge) should be considered as a conservative lower estimate. Figure 3 shows the contour plot of the modern merger rate as a function of the clustering parameter δ_{PBH} and the velocity dispersion σ in the cluster. One can see that there exists a region of parameters near $\delta_{\text{PBH}} \gtrsim 1$, where one can explain all dark matter in terms of PBHs with mass $\sim 10 M_{\odot}$. However, many other constraints imposed on the PBHs of these masses exclude this possibility. With a significant increase in the clustering parameter $\delta_{\text{PBH}} \gg 1$, the merger rate is determined by binaries with nearly circular orbits. Moreover, increasing δ_{PBH} leads to an enhancement of the modern merger rate, as can also be seen in Fig. 2. Thus, the early clustering effect makes it virtually impossible to relax the gravitational-wave constraints to the level where all dark matter could consist of PBHs. This conclusion is also consistent with the results obtained in Ref. [42]. However it should be noted, that in the region $\delta_{\text{PBH}} \gtrsim 1$ and $\sigma \gtrsim 100 \text{ km/s}$, the merger rate is exponentially

suppressed (according to Eq. (5.2)), since in this case all binary systems are soft and undergo destruction. In the opposite limit $\delta_{\text{PBH}} \ll 1$ clusters are formed at enough late stages, that significantly reduces the efficiency of perturbations on binary systems (see Eq. (4.5)), and we return to the situation of PBHs unclustered at birth, for which the standard constraints on their fraction in dark matter f are valid.

6 Stochastic gravitational wave background

In the previous section the behavior of the PBH merger rate on cosmological time scales was considered. However individual events of black hole mergers at high redshifts may remain observationally unresolved, nevertheless their total contribution to the energy density of gravitational waves in the Universe can be significant. In this section, we discuss the impact of our results on the characteristics of the GW background, which is traditionally described by the relative spectral energy density [47]

$$\Omega_{\text{gw}} = \frac{1}{\rho_{\text{crit}} c^2} \frac{d\rho_{\text{gw}}}{d \ln \nu} = \frac{1}{\rho_{\text{crit}} c^2} \int_0^\infty dz \frac{\mathcal{R}(z)}{H(z)(1+z)^2} \frac{dE_{\text{gw}}}{d \ln \nu_s}, \quad (6.1)$$

where $\nu_s = (1+z)\nu$ is the gravitational wave frequency in the source system and $dE_{\text{gw}}/d \ln \nu_s$ is the gravitational wave energy emitted during the merger of a binary black hole in a logarithmic bin of frequency. In this paper we use the inspiral-merger-ringdown energy spectrum [48, 49]. In fact, Eq. (6.1) is the sum of the energy released from all merger events summed over all redshifts. It should be noted that the analysis of the stochastic GW background from PBH mergers has also been studied in Refs. [44, 50–57].

First, we parametrize the redshift evolution of the merger rate as $\mathcal{R} = \mathcal{R}_0(1+z)^\kappa$ and derive an analytic expression for the GW background, which will show the main idea of this section. For these purposes it is enough for us to consider only the inspiral phase of a binary black hole whose energy spectrum is [58]

$$\frac{dE}{d \ln \nu_s} = \frac{\pi^{2/3}}{3G} (GM_c)^{5/2} \nu_s^{2/3}, \quad (6.2)$$

where $M_c = (m_1 m_2)^{3/5} / (m_1 + m_2)^{1/5}$ is the chirp mass and in our case of equal masses black holes $M_c = m/2^{1/5}$. We will assume that the inspiral phase, described by Eq. (6.2), continues up to some maximum frequency ν_{max} and then $dE/d \ln \nu_s$ drops to zero. Such simplified model corresponds to the instantaneous formation of a new merged black hole after reaching ν_{max} . Then the amplitude of the GW background depends on the frequency as follows

$$\begin{aligned} \Omega_{\text{gw}} &= A \nu^{2/3} \frac{\mathcal{R}_0 \pi^{2/3} (Gm)^{5/3}}{3\sqrt{2} G \rho_{\text{crit}} c^2} \int_0^{(\nu_{\text{max}}/\nu)^{-1}} \frac{(1+z)^{\kappa+2/3}}{(1+z)^2 H(z)} dz \\ &\approx \frac{A \mathcal{R}_0 \pi^{2/3} (Gm)^{5/3} \nu^{2/3}}{3\sqrt{2} G \rho_{\text{crit}} c^2 H_0 \sqrt{\Omega_M} (\kappa - 11/6)} \left[\left(\frac{\nu_{\text{max}}}{\nu} \right)^{\kappa-11/6} - 1 \right], \end{aligned} \quad (6.3)$$

where in the second equality we used the Hubble rate approximation $H(z) \approx H_0 \sqrt{\Omega_M (1+z)^3}$, which holds already at redshifts $z > 1$. The introduced constant A compensates for the deviations of the simplified spectrum (6.2) from the realistic case and will be determined numerically in the further analysis. It can be seen that at $\kappa < 11/6$ the second term in

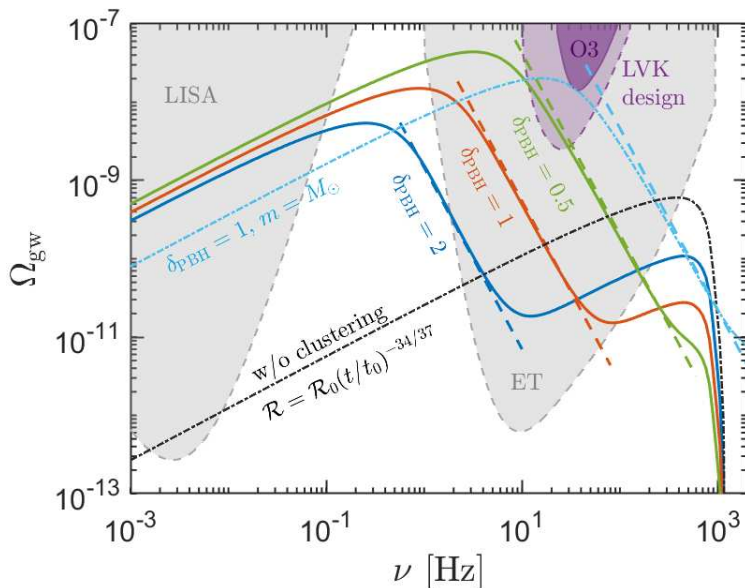


Figure 4. Spectral energy density of the stochastic gravitational-wave background from mergers of PBHs with $m = 10 M_{\odot}$ mass for different values of the clustering parameter δ_{PBH} and $\sigma = 10 \text{ km s}^{-1}$, and $f = 1$ in Eq. (5.5). The dotted line shows the analytic approximation is given by Eq. (6.5), with the minimum plotting frequency determined by ν_{sup} from Eq. (6.6). The dash-dotted line shows the case of the Poisson (with no initial clustering) distribution of PBHs normalized such that the modern merger rate $\mathcal{R}_0 = 10 \text{ Gpc}^{-3} \text{ yr}^{-1}$. The shaded areas show the projected sensitivity of some future GW detectors, as well as the upper limit from the O3 run results [59].

brackets of Eq. (6.3) is the dominant one, which leads to the classical power-law spectrum of $\Omega_{\text{gw}} \propto \nu^{2/3}$, which is characteristic for black hole mergers. However, when $\kappa > 11/6$, the spectral slope deviates from the canonical scaling, taking the form $\Omega_{\text{gw}} \propto \nu^{5/2-\kappa}$. Note that earlier work [57] also showed a direct connection between the spectral index of the GW background and the redshift evolution of black holes merger rate. Of particular interest is the case of sufficiently fast growth of the merger rate with redshift $\kappa > 5/2$, when the spectral slope of the GW energy density becomes negative — this is the case realized in our work.

Figure 4 shows the stochastic GW background calculated using the merge rate (5.5) for different values of the clustering parameter δ_{PBH} . As can be seen from the graph, the spectral index takes negative values in a certain frequency range. We now obtain an analytical approximation for Ω_{gw} in this region. As shown in the previous section, during the period of active perturbation of PBH binaries the merger rate evolves according to Eq. (5.6) as $\mathcal{R} \propto (t/t_0)^{-45/14}$, which corresponds to the following dependence on the redshift z

$$\mathcal{R} = \mathcal{R}_0 \left(\frac{2}{3H_0 t_0 \sqrt{\Omega_M}} \right)^{-45/14} (1+z)^{135/28}, \quad (6.4)$$

where, as before, we have used the dust stage approximation $t(z) = 2/3H(z)$, since we are interested in the high redshift limit. Taking the maximum frequency of the GW in Eq. (6.3) as $\nu_{\text{max}} = 0.057 c^3/Gm$ (corresponding to the spectrum break $dE_{\text{gw}}/d \ln \nu_s$ at higher frequencies [48]), then good agreement with numerical calculations is obtained with

the estimate $A \sim 1$:

$$\Omega_{\text{gw}} \approx 9.7 \times 10^{-7} f \delta_{\text{PBH}}^{-44/7} \left(\frac{\sigma}{10 \text{ km s}^{-1}} \right)^{29/14} \left(\frac{m}{M_{\odot}} \right)^{-13/4} \left(\frac{\nu}{10 \text{ Hz}} \right)^{-65/28}. \quad (6.5)$$

This dependence is shown by dotted lines in Fig. 4. The suppression of the merger rate begins at time t_{sup} , defined by Eq. (4.5), so the corresponding GW frequency experiences a redshift $\nu_{\text{sup}} = \nu_{\text{max}}/(1 + z_{\text{sup}})$:

$$\begin{aligned} \nu_{\text{sup}} &= \nu_{\text{max}} \left(\frac{3H_0 t_{\text{sup}} \sqrt{\Omega_M}}{2} \right)^{2/3} \\ &\approx 2.2 \delta_{\text{PBH}}^{-80/41} \left(\frac{\sigma}{10 \text{ km s}^{-1}} \right)^{74/123} \left(\frac{m}{M_{\odot}} \right)^{-161/123} \text{ Hz}. \end{aligned} \quad (6.6)$$

Thus, in the frequency range $\nu > \nu_{\text{sup}}$, the spectral density of gravitational waves is characterized by a negative slope $\Omega_{\text{gw}} \propto \nu^{-65/28}$. At lower frequencies, the classical dependence $\Omega_{\text{gw}} \propto \nu^{2/3}$, typical for merging black hole binaries. However, in the frequency band of space-based interferometers like LISA, a strong excess of Ω_{gw} is expected compared to the case of PBHs with Poisson spatial distribution (and perhaps even over astrophysical sources). Let us now discuss the frequencies ~ 100 Hz. Provided that PBHs of tens solar masses do not dominate the observed GW events, then in these frequencies the main contribution to the GW background comes from mergers of black holes of stellar origin [50], which also leads to the standard dependence $\Omega_{\text{gw}} \propto \nu^{2/3}$. However, a comprehensive analysis of the GW background taking into account various PBHs clustering scenarios and the contribution of astrophysical sources is beyond the scope of this paper and will be addressed in a separate article. Nevertheless, as can be seen from Fig. 4, there is parameter region in which future GW detectors will be able to test the possibility of PBHs clustering.

7 Conclusion

The paper investigated the influence of the initial clustering of PBHs on the dynamics of their mergers. It was shown that a significant part of the binaries are characterized by sufficiently wide orbits and small angular momenta, and therefore they are perturbed in the dense environment of the cluster. This process leads to an effective “elimination” of such binaries from the merger process due to a significant increase of their coalescence time or even destruction. At the same time, rare close binaries are more likely to avoid perturbations and therefore continue to merge. Such a change in the distribution of the PBH binaries orbital parameters causes a suppression of the merger rate starting from the time t_{sup} determined by Eq. (4.5), these results are shown in Fig. 2. In the epoch of active binaries perturbation, the merger rate depends on the cosmological time as $\mathcal{R} \propto t^{-45/14}$ (in accordance with Eq. (5.6)). Which differs significantly from the case of a Poisson (initially non-clustered) distribution of PBHs in the space $\mathcal{R} \propto t^{-34/37}$. The study of the redshift evolution of black holes merger rate is one of the target for the next generation of gravitational wave detectors. Therefore, future observations will be able not only to verify the existence of PBHs, but also to reconstruct the features of their initial spatial distribution, which will make it possible to identify the most plausible scenarios for their formation. The absence of GW signals at high redshifts, in turn, will impose strict constraints on the parameters of PBHs formation models.

On the other hand, if direct detection of GW transients from black hole mergers at large redshifts turns out to be observationally difficult, their overall contribution remains significant as the integral effect on the gravitational wave energy in the Universe. Therefore, in Section 6 we analyze the impact of our results for the stochastic GW background. We demonstrate that a rapid growth in the black hole merger rate with redshift causes spectral features in the GW energy density, as illustrated in Fig. 4. Specifically, when the merger rate is scaled with time as $\mathcal{R} \propto t^{-45/14}$, the stochastic GW background depends on the frequency $\Omega_{\text{gw}} \propto \nu^{-65/28}$ in the frequency range above ν_{sup} given by Eq. (6.6). This is radically different from the traditional expectation of $\Omega_{\text{gw}} \propto \nu^{2/3}$ for black hole mergers. The obtained results provide an additional possibility for experimentally testing PBH clustering scenarios.

Acknowledgment

The work was funded by the Ministry of Science and Higher Education of the Russian Federation, Project "New Phenomena in Particle Physics and the Early Universe" FSWU-2023-0073

References

- [1] Y.B. Zel'dovich and I.D. Novikov, *The Hypothesis of Cores Retarded during Expansion and the Hot Cosmological Model*, *Sov. Astron.* **10** (1967) 602.
- [2] S. Hawking, *Gravitationally collapsed objects of very low mass*, *Mon. Not. R. Astron. Soc.* **152** (1971) 75.
- [3] KAGRA, VIRGO, LIGO SCIENTIFIC collaboration, *Population of Merging Compact Binaries Inferred Using Gravitational Waves through GWTC-3*, *Phys. Rev. X* **13** (2023) 011048 [[2111.03634](#)].
- [4] KAGRA, VIRGO, LIGO SCIENTIFIC collaboration, *GWTC-3: Compact Binary Coalescences Observed by LIGO and Virgo during the Second Part of the Third Observing Run*, *Phys. Rev. X* **13** (2023) 041039 [[2111.03606](#)].
- [5] S. Bird, I. Cholis, J.B. Muñoz, Y. Ali-Haïmoud, M. Kamionkowski, E.D. Kovetz et al., *Did LIGO detect dark matter?*, *Phys. Rev. Lett.* **116** (2016) 201301 [[1603.00464](#)].
- [6] M. Sasaki, T. Suyama, T. Tanaka and S. Yokoyama, *Primordial Black Hole Scenario for the Gravitational-Wave Event GW150914*, *Phys. Rev. Lett.* **117** (2016) 061101 [[1603.08338](#)].
- [7] S. Clesse and J. García-Bellido, *The clustering of massive Primordial Black Holes as Dark Matter: measuring their mass distribution with Advanced LIGO*, *Phys. Dark Univ.* **15** (2017) 142 [[1603.05234](#)].
- [8] S. Blinnikov, A. Dolgov, N.K. Porayko and K. Postnov, *Solving puzzles of GW150914 by primordial black holes*, *JCAP* **11** (2016) 036 [[1611.00541](#)].
- [9] Y. Ali-Haïmoud, E.D. Kovetz and M. Kamionkowski, *Merger rate of primordial black-hole binaries*, *Phys. Rev. D* **96** (2017) 123523 [[1709.06576](#)].
- [10] M. Raidal, C. Spethmann, V. Vaskonen and H. Veermäe, *Formation and Evolution of Primordial Black Hole Binaries in the Early Universe*, *JCAP* **02** (2019) 018 [[1812.01930](#)].
- [11] V. De Luca, G. Franciolini, P. Pani and A. Riotto, *Primordial Black Holes Confront LIGO/Virgo data: Current situation*, *JCAP* **06** (2020) 044 [[2005.05641](#)].
- [12] G. Hütsi, M. Raidal, V. Vaskonen and H. Veermäe, *Two populations of LIGO-Virgo black holes*, *JCAP* **03** (2021) 068 [[2012.02786](#)].

- [13] B. Carr, K. Kohri, Y. Sendouda and J. Yokoyama, *Constraints on primordial black holes*, *Rept. Prog. Phys.* **84** (2021) 116902 [[2002.12778](#)].
- [14] T. Nakamura, M. Sasaki, T. Tanaka and K.S. Thorne, *Gravitational waves from coalescing black hole MACHO binaries*, *Astrophys. J. Lett.* **487** (1997) L139 [[astro-ph/9708060](#)].
- [15] B.J. Kavanagh, D. Gaggero and G. Bertone, *Merger rate of a subdominant population of primordial black holes*, *Phys. Rev. D* **98** (2018) 023536 [[1805.09034](#)].
- [16] S. Pilipenko, M. Tkachev and P. Ivanov, *Evolution of a primordial binary black hole due to interaction with cold dark matter and the formation rate of gravitational wave events*, *Phys. Rev. D* **105** (2022) 123504 [[2205.10792](#)].
- [17] P. Jangra, B.J. Kavanagh and J.M. Diego, *Impact of dark matter spikes on the merger rates of Primordial Black Holes*, *JCAP* **11** (2023) 069 [[2304.05892](#)].
- [18] V.D. Stasenko and Y.N. Eroshenko, *Mergers of Binary Primordial Black Holes in Evolving Dark Matter Halos*, *Astron. Lett.* **50** (2024) 431 [[2412.20859](#)].
- [19] V. Vaskonen and H. Veermäe, *Lower bound on the primordial black hole merger rate*, *Phys. Rev. D* **101** (2020) 043015 [[1908.09752](#)].
- [20] K. Jedamzik, *Primordial Black Hole Dark Matter and the LIGO/Virgo observations*, *JCAP* **09** (2020) 022 [[2006.11172](#)].
- [21] M. Tkachev, S. Pilipenko and G. Yepes, *Dark Matter Simulations with Primordial Black Holes in the Early Universe*, *Mon. Not. Roy. Astron. Soc.* **499** (2020) 4854 [[2009.07813](#)].
- [22] V. Stasenko and K. Belotsky, *Influence of early dark matter haloes on the primordial black holes merger rate*, *Mon. Not. Roy. Astron. Soc.* **526** (2023) 4308 [[2307.12924](#)].
- [23] V. Stasenko, *Redshift evolution of primordial black hole merger rate*, *Phys. Rev. D* **109** (2024) 123546 [[2403.11325](#)].
- [24] M.S. Delos, A. Rantala, S. Young and F. Schmidt, *Structure formation with primordial black holes: collisional dynamics, binaries, and gravitational waves*, *JCAP* **12** (2024) 005 [[2410.01876](#)].
- [25] P. Amaro-Seoane, H. Audley, S. Babak, J. Baker, E. Barausse, P. Bender et al., *Laser interferometer space antenna*, *arXiv preprint arXiv:1702.00786* (2017) .
- [26] TIANQIN collaboration, *TianQin: a space-borne gravitational wave detector*, *Class. Quant. Grav.* **33** (2016) 035010 [[1512.02076](#)].
- [27] ET collaboration, *Science Case for the Einstein Telescope*, *JCAP* **03** (2020) 050 [[1912.02622](#)].
- [28] A. Abac et al., *The Science of the Einstein Telescope*, **2503.12263**.
- [29] S.G. Rubin, A.S. Sakharov and M.Y. Khlopov, *The Formation of primary galactic nuclei during phase transitions in the early universe*, *J. Exp. Theor. Phys.* **91** (2001) 921 [[hep-ph/0106187](#)].
- [30] M.Y. Khlopov, S.G. Rubin and A.S. Sakharov, *Primordial structure of massive black hole clusters*, *Astropart. Phys.* **23** (2005) 265 [[astro-ph/0401532](#)].
- [31] S. Young and C.T. Byrnes, *Signatures of non-gaussianity in the isocurvature modes of primordial black hole dark matter*, *JCAP* **04** (2015) 034 [[1503.01505](#)].
- [32] Y. Tada and S. Yokoyama, *Primordial black holes as biased tracers*, *Phys. Rev. D* **91** (2015) 123534 [[1502.01124](#)].
- [33] K.M. Belotsky, V.I. Dokuchaev, Y.N. Eroshenko, E.A. Esipova, M.Y. Khlopov, L.A. Khromykh et al., *Clusters of primordial black holes*, *Eur. Phys. J. C* **79** (2019) 246 [[1807.06590](#)].
- [34] V. Desjacques and A. Riotto, *Spatial clustering of primordial black holes*, *Phys. Rev. D* **98** (2018) 123533 [[1806.10414](#)].

- [35] T. Suyama and S. Yokoyama, *Clustering of primordial black holes with non-Gaussian initial fluctuations*, *PTEP* **2019** (2019) 103E02 [[1906.04958](#)].
- [36] Q. Ding, T. Nakama, J. Silk and Y. Wang, *Detectability of Gravitational Waves from the Coalescence of Massive Primordial Black Holes with Initial Clustering*, *Phys. Rev. D* **100** (2019) 103003 [[1903.07337](#)].
- [37] E.W. Kolb and I.I. Tkachev, *Large amplitude isothermal fluctuations and high density dark matter clumps*, *Phys. Rev. D* **50** (1994) 769 [[astro-ph/9403011](#)].
- [38] PLANCK collaboration, *Planck 2018 results. VI. Cosmological parameters*, *Astron. Astrophys.* **641** (2020) A6 [[1807.06209](#)].
- [39] P.C. Peters, *Gravitational radiation and the motion of two point masses*, *Phys. Rev.* **136** (1964) B1224.
- [40] D.C. Heggie, *Binary evolution in stellar dynamics.*, *Mon. Not. R. Astron. Soc.* **173** (1975) 729.
- [41] J.G. Hills, *Encounters between binary and single stars and their effect on the dynamical evolution of stellar systems.*, *Astron. J.* **80** (1975) 809.
- [42] T. Bringmann, P.F. Depta, V. Domcke and K. Schmidt-Hoberg, *Towards closing the window of primordial black holes as dark matter: The case of large clustering*, *Phys. Rev. D* **99** (2019) 063532 [[1808.05910](#)].
- [43] S. Young and C.T. Byrnes, *Initial clustering and the primordial black hole merger rate*, *JCAP* **03** (2020) 004 [[1910.06077](#)].
- [44] V. Atal, A. Sanglas and N. Triantafyllou, *LIGO/Virgo black holes and dark matter: The effect of spatial clustering*, *JCAP* **11** (2020) 036 [[2007.07212](#)].
- [45] F. Crescimbeni, V. Desjacques, G. Franciolini, A. Iannicari, A.J. Iovino, G. Perna et al., *The irrelevance of primordial black hole clustering in the LVK mass range*, *JCAP* **05** (2025) 001 [[2502.01617](#)].
- [46] G. Franciolini, K. Kritos, E. Berti and J. Silk, *Primordial black hole mergers from three-body interactions*, *Phys. Rev. D* **106** (2022) 083529 [[2205.15340](#)].
- [47] E.S. Phinney, *A Practical theorem on gravitational wave backgrounds*, [astro-ph/0108028](#).
- [48] P. Ajith et al., *A Template bank for gravitational waveforms from coalescing binary black holes. I. Non-spinning binaries*, *Phys. Rev. D* **77** (2008) 104017 [[0710.2335](#)].
- [49] P. Ajith et al., *Inspiral-merger-ringdown waveforms for black-hole binaries with non-precessing spins*, *Phys. Rev. Lett.* **106** (2011) 241101 [[0909.2867](#)].
- [50] V. Mandic, S. Bird and I. Cholis, *Stochastic Gravitational-Wave Background due to Primordial Binary Black Hole Mergers*, *Phys. Rev. Lett.* **117** (2016) 201102 [[1608.06699](#)].
- [51] S. Wang, Y.-F. Wang, Q.-G. Huang and T.G.F. Li, *Constraints on the Primordial Black Hole Abundance from the First Advanced LIGO Observation Run Using the Stochastic Gravitational-Wave Background*, *Phys. Rev. Lett.* **120** (2018) 191102 [[1610.08725](#)].
- [52] S. Clesse and J. García-Bellido, *Detecting the gravitational wave background from primordial black hole dark matter*, *Phys. Dark Univ.* **18** (2017) 105 [[1610.08479](#)].
- [53] S.S. Bavera, G. Franciolini, G. Cusin, A. Riotto, M. Zevin and T. Fragos, *Stochastic gravitational-wave background as a tool for investigating multi-channel astrophysical and primordial black-hole mergers*, *Astron. Astrophys.* **660** (2022) A26 [[2109.05836](#)].
- [54] S. Mukherjee and J. Silk, *Can we distinguish astrophysical from primordial black holes via the stochastic gravitational wave background?*, *Mon. Not. Roy. Astron. Soc.* **506** (2021) 3977 [[2105.11139](#)].

- [55] J. García-Bellido, S. Jaraba and S. Kuroyanagi, *The stochastic gravitational wave background from close hyperbolic encounters of primordial black holes in dense clusters*, *Phys. Dark Univ.* **36** (2022) 101009 [[2109.11376](#)].
- [56] M. Braglia, J. Garcia-Bellido and S. Kuroyanagi, *Testing Primordial Black Holes with multi-band observations of the stochastic gravitational wave background*, *JCAP* **12** (2021) 012 [[2110.07488](#)].
- [57] V. Atal, J.J. Blanco-Pillado, A. Sanglas and N. Triantafyllou, *Constraining changes in the merger history of BH and PBH binaries with the stochastic gravitational wave background*, *Phys. Rev. D* **105** (2022) 123522 [[2201.12218](#)].
- [58] M. Maggiore, *Gravitational Waves. Vol. 1: Theory and Experiments*, Oxford University Press (2007), [10.1093/acprof:oso/9780198570745.001.0001](#).
- [59] KAGRA, VIRGO, LIGO SCIENTIFIC collaboration, *Upper limits on the isotropic gravitational-wave background from Advanced LIGO and Advanced Virgo's third observing run*, *Phys. Rev. D* **104** (2021) 022004 [[2101.12130](#)].